Vacuum 149 (2018) 96–100

Contents lists available at ScienceDirect

Vacuum

journal homepage: www.elsevier.com/locate/vacuum

Investigation on microstructure of electron beam welded WC-Co/40Cr joints

Guoqing Chen*, Xi Shu, Junpeng Liu, Bo Zhang, Binggang Zhang, Jicai Feng

State Key Laboratory of Advanced Welding and Joining, Harbin Institute of Technology, Harbin 150001, China

A R T I C L E I N F O

Article history:
Received 26 September 2017
Received in revised form
11 November 2017
Accepted 12 December 2017
Available online 13 December 2017

Keywords:
Electron beam welding
WC-Co cemented carbide
40Cr steel
η phase

A B S T R A C T

The electron beam welding of WC-Co cemented carbide and 40Cr steel was studied in this paper. The mechanism of microstructure evolution in the joint was analyzed. The weld was mainly composed of (Fe, C) martensite and η phases consisted of Fe_3W_3C. But the eutectic reaction occurred in the weld when the heat input was large, and then eutectic phases composed of (Fe, C) and η phases were generated. With the decrease of heat input, the content of η phase would decline.

1. Introduction

With the rapid development of the industrial process, more and more machinery and equipment are used in the mining operation, and the efficiency and costs are directly affected by the quality of the cutter. At present, the cutting of the carbide head composed of cemented carbide is usually combined with the steel base to save the cost [1]. Brazing was usually used to welding cemented carbide and steel in the traditional process, but the joint would be in low strength under high temperature and short service life. Cemented carbide and steel can be welded by arc welding, but the heat affected zone would be large, which had a negative effect on the performance of the joint.

The joints of cemented carbide and steel can be obtained by adding Ni, Ni-Fe or Ni-Fe-C interlayers. Few η phases (Fe_3W_3C) existed in the interface using Ni-Fe-C while it would be more by adding Ni and Ni-Fe [2,3]. Cracks and pores are the two main defects in laser welding of cemented carbide and invar alloy. The cracks always occurred in the cemented carbide while there were no cracks found in the weld bead [4]. Lower residual stress maximum values, crack-free and non-porous joints of cemented carbide and steel were obtained with pre-heating and post heat treatment using laser beam welding [5]. Joints with good performance could be obtained by electron beam welding (EBW) with or without interlayers, and the maximum tensile strength was 560 MPa using interlayers [6,7]. Diffusion welding is also a method to realize the connection of cemented carbide and steel, but the tensile strengths of the joints were not satisfactory [8–10]. Joints of dissimilar materials can be obtained by brazing method. Cemented carbide and steel can be welded using Cu-Zn-Ni [11], Cu-Ni [12], Cu-Mn-Zn [13] and Cu-Ag [14] with no cracks existed in the joints. However, the tensile strengths of the joints were generally not high because the base materials did not melt and the solders were low in strength.

In the industrial applications, WC-Co cemented carbides and steel are usually welded together to improve production efficiency and reduce costs due to the cemented carbides are expensive. EBW is especially suitable for welding dissimilar materials due to its unique heat transfer mechanism and pure welding environment. Compared with other fusion welding methods, EBW has the advantages of low heat input, small welding deformation, high energy density and high penetration. In the present work, EBW of WC-Co cemented carbide and steel with annular weld was carried out to provide a detailed description of the microstructure transformation characterization.

2. Materials and methods

WC-Co cemented carbide (Φ35 mm × 20 mm with sink hole Φ20 mm × 4 mm) and 40Cr steel with size of Φ20 mm × 4 mm

* Corresponding author.
E-mail address: chenguoqing@hit.edu.cn (G. Chen).

https://doi.org/10.1016/j.vacuum.2017.12.012
0042-207X/

Table 1
Chemical composition of 40Cr steel (wt.%).

C	Si	Mn	Cr	Ni	Cu	P	S	Fe
0.37–0.44	0.17–0.37	0.5–0.8	0.8–1.1	≤0.3	≤0.03	≤0.035	≤0.035	Bal.

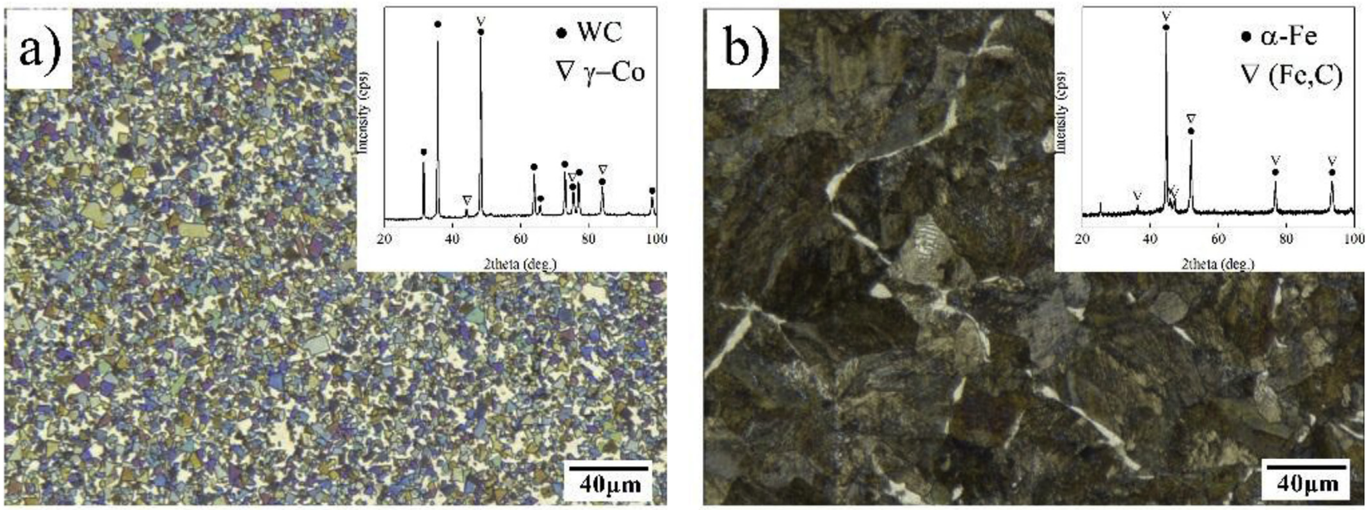

Fig. 1. The chemical analyses of the base metals. a) WC-Co. b) 40Cr.

were used in the experiment. The WC-Co base metal is composed of WC (70 wt.%) and Co (30 wt.%) and the chemical composition of 40Cr steel given by the supplier in wt.% is shown in Table 1. The chemical analyses of the base metals are shown in Fig. 1. It can be seen that the cemented carbide contains only WC and γ-Co, while the 40Cr steel mainly consists of α-Fe and (Fe, C) phases. WC particles are distributed in the shape of triangular and rectangular. The assembly diagram of EBW of WC-Co and 40Cr was shown in Fig. 2. The electron beam was perpendicular to the upper surface of the base metal, moving along the annular interface of WC-Co and 40Cr to obtain EBW joints.

For microscopic observation, the samples were studied under optical microscope (VHX-1000) and scanning electron microscope (SEM) (Quanta 200FEG). Distribution of chemical elements was analyzed by using EDS integrated in the SEM.

Specimens were cut and polished using a series of SiC emery papers from 200 to 5000 grit size in succession with water as the coolant, followed by fine polishing using 0.5 μm diamond paste in a velvet cloth disc. To reveal the microstructure, 2%HNO_3+C_2H_5OH were used as the etchants. The etched samples were studied under optical microscope and polished samples and fracture were studied under scanning electron microscope (SEM). Distribution of chemical elements was analyzed by using EDS. The parameters used in the experiment were shown in Table 2, where U represented accelerating voltage, I_b was beam current, v was welding speed and d represented the deviation to steel.

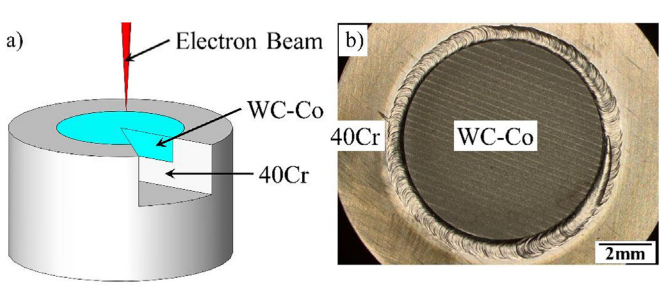

Fig. 2. EBW process of WC-Co/steel. a) Schematic diagram. b) Appearance of the weld.

3. Results and discussion

3.1. Weld microstructures

Fig. 3 showed the cross-section of the EB joints under different heat input. The molten pool was mainly consisted of steel because the focus of electron beam was deflected to 40Cr side. The joint cannot achieve full penetration due to insufficient heat input when I_b = 16 mA. Only an effective connection could be formed at the upper part of the joint, while the middle and lower parts of the 40Cr were not completely melted. But no macro cracks were found in the weld and interface. The penetration depth was too large under 22 mA and resulted in the cracks through the whole interface. The joint was melted in an appropriate penetration depth and the interface was effectively connected when beam current was 18 mA, but there were obvious macro cracks in the weld.

Spiking were found in all joints due to the semi-penetration structure. As the energy of the electron beam is relatively concentrated, the metal near the electron beam reaches the boiling point instantaneously, and the metallic vapor cannot escape in time under the fast cooling rate. Finally, the spiking defect was formed after cooling [15]. The differences of thermodynamic properties between WC-Co cemented carbide and 40Cr would result in cracks in the joint.

The SEM images clearly demonstrate that heat input has large

Table 2
Process parameters of EBW of WC-Co and 40Cr.

U/kV	I_b/mA	v/mm·s^{-1}	d/mm
55	16–22	3	0.2